**Electrochemical Sensors**

DOI: 10.1002/anie.200700341

# Electrochemical Sensor with Record Performance Characteristics

*Arkady A. Karyakin,* Elena A. Puganova, Ivan A. Bolshakov, and Elena E. Karyakina*

Accessing the limiting performance characteristics of sensors is possible by means of their miniaturization. Microelectrodes demonstrate a significantly improved sensitivity and signal-to-noise ratio, the latter being inversely proportional to the electrode radius.[1–3] However, a decrease in the electrode dimensions limits the sensor response to very low current values. To avoid this problem, it is possible to use microelectrode arrays, which are commonly produced by creating an insulating layer on a macroelectrode surface and then making holes in this layer.[4–7]

To develop a sensor with improved performance characteristics, we propose nanostructuring of a highly active electrocatalyst onto an inert electrode support. Since the reduction—or the oxidation—of the analyte on the support is negligible, the species diffuses to the place where it is being consumed, namely, to the electrocatalyst islands, which are thus expected to behave as nanoelectrodes. Herein we report a hydrogen peroxide sensor composed of nanostructured Prussian Blue on an inert carbon surface. This electrochemical sensor displayed record performance in the flow-injection mode, thereby exhibiting a linear calibration range that extended over seven orders of magnitude of $H_2O_2$ concentration, with its lower limit being $1\times10^{-9}\,\text{mol}\,\text{L}^{-1}$ $H_2O_2$ (i.e., 0.03 ppb). These results represent a record in electroanalysis.

We reported that Prussian Blue is the most advantageous electrocatalyst for hydrogen peroxide reduction.[8–10] Prussian-Blue-modified electrodes are characterized by an electrochemical rate constant that is up to three orders of magnitude higher than that observed with the most widely used platinum electrodes. The deposition of Prussian Blue through liquid-crystalline templates was carried out according to the most common approaches for nanostructuring,[11–13] thus obtaining a nanostructured inorganic polycrystal.[14]

The AFM image in Figure 1a shows that the Prussian-Blue layer grown without templates covers the surface completely. The inorganic film itself exhibits a polycrystalline structure, with crystalline dimensions of less than 100 nm. To estimate the thickness of the Prussian-Blue layer, a part of the film was removed from the electrode surface by using a droplet of an alkaline solution, which is known to solubilize ferric ferrocyanide (Prussian Blue). The layer thickness, determined by AFM, was found to be about 60–80 nm. An increase in the deposition time results in thicker—but less regular—polycrystalline structures.[10]

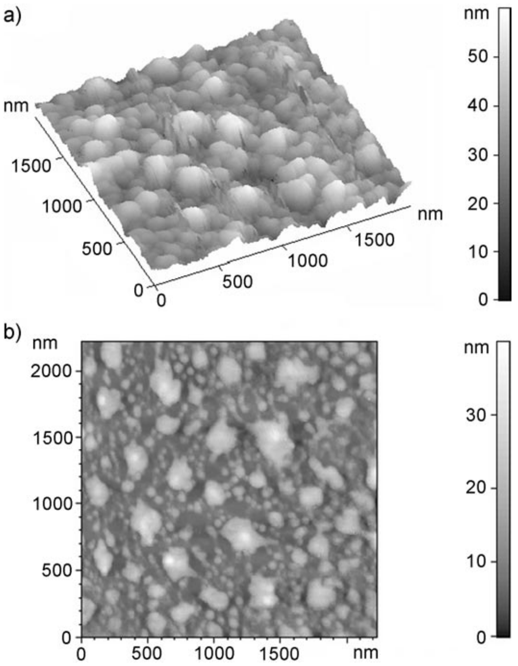

***Figure 1.*** AFM images of Prussian-Blue-modified monocrystalline graphite: a) conventional Prussian Blue, deposited without templates, b) Prussian Blue electrochemically deposited through a vinyltriethoxysilane sol template.

The best results in terms of nanostructuring were obtained with vinyltriethoxysilane-based sol prepared from acetonitrile. An AFM image of Prussian Blue grown through this template is shown in Figure 1b. Deposition through the alkoxysilane sol results in an archipelago of structures. The surrounding smooth area can be attributed to the blank surface, taking into account the thickness of the Prussian-Blue film grown without templates.

The optimal geometry of the micro- and nanoelectrode arrays can be found considering the diffusion profiles of the analyte at the electrode surface. An array of hemispherical ultramicroelectrodes (Figure 2) is the best model for nano-

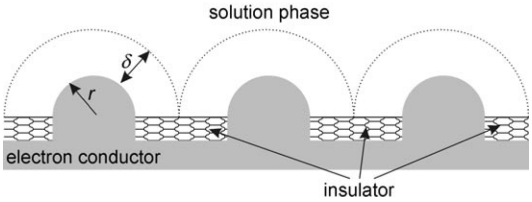

***Figure 2.*** Array of hemispherical microelectrodes (schematic).

---

[*] Prof. A. A. Karyakin, Dr. E. A. Puganova, I. A. Bolshakov,
Dr. E. E. Karyakina
Chemistry Faculty, M. V. Lomonosov
Moscow State University, 119991, Moscow (Russia)
Fax: (+7) 495-939-4675
E-mail: aak@analyt.chem.msu.ru

Supporting information for this article is available on the WWW under http://www.angewandte.org or from the author.

structured electrocatalysts. Assuming that the analyte concentration at a distance $\delta$ from the electrode surface tends to its bulk value, the best performance characteristics of micro- and nanoelectrode arrays can be accessed if the individual electrodes are separated by a distance $2\delta$ (Figure 2). Indeed, at smaller distances, the individual electrodes interfere with each other, and the diffusion profiles are not hemispherical. A larger separation, on the other hand, results in a decreased current density, which reduces both the sensitivity and the signal-to-noise ratio of the resulting sensor.

The value of $\delta$ for hemispherical ultramicroelectrodes can be calculated from the relations for the steady-state current.[1] We found that $\delta$ is equal to the radius ($r$) of the ultramicroelectrode; hence, the optimal configuration for an array of hemispherical ultramicroelectrodes is that with an electrode separation equal to their diameter. The nanostructured Prussian Blue shown in Figure 1 b is roughly reminiscent of such an optimal configuration, which allows us to expect limiting-performance characteristics for the corresponding sensor.

Sensor performance characteristics were investigated in a flow-injection system equipped with a flow-through wall-jet cell. Flow-through electrodes are known to provide the most reproducible and stable hydrodynamics, which are necessary to investigate sensor response in a wide concentration range. A wall-jet electrode consists of a jet of solution issued from a circular nozzle and allowed to impinge normally on a working disk electrode.

Forced-hydrodynamic techniques—including flow-through electrodes—create specific depolarizer concentration profiles, which include the Nernst's (diffusion) layer at the electrode surface. In this layer mass transport is known to occur only by diffusion.[1]

The diffusion-layer thickness of a wall-jet electrode, which was first estimated by Yamada and Matsuda,[15] reaches its lowermost value in the center of the impinging jet; however, this value is not equal to zero, as originally assumed by these authors.[15] The correct value can be obtained from the limiting case, in which the electrode is much thinner than the nozzle.[16,17] The lower limit of the diffusion-layer thickness of the wall-jet electrode used herein was estimated to be 4.5–5 μm, which is one to two orders of magnitude larger than the dimensions of Prussian-Blue clusters (Figure 1 b). Hence, mass transport at the electrode surface mainly takes place by diffusion to the nanoelectrode arrays, which results in improved analytical characteristics of the sensor. Moreover, for nanostructured Prussian Blue, the signal-to-noise ratio was independently found to be almost one order of magnitude higher than that of the unstructured electrocatalyst.

Flow-injection analysis (FIA) is based on the injection of a liquid sample into a moving, nonsegmented, continuous carrier stream of a suitable liquid. The FIA response is a current peak, whose height, multiplied by the dispersion coefficient (which in our experiments has value of approximately two), is equal to the steady-state-current response obtained through a continuous flow of the analyte.[18] In FIA—relative to batch or continuous-flow analysis—the response (peak current) is better recognizable from the baseline noise. This feature is advantageous for electroanalysis, as it allows reproducible detection at low analyte concentrations.

The calibration plot for $H_2O_2$ in the flow-injection mode (with the use of nanostructured Prussian Blue as a detector) is presented in Figure 3. The slope of the linear calibration range is $0.7\,\mathrm{A\,L\,mol^{-1}\,cm^{-2}}$, which is similar to that of conventional (unstructured) Prussian Blue (namely, $(0.6 \pm 0.1)\,\mathrm{A\,L\,mol^{-1}\,cm^{-2}}$). Hence, we succeeded in forming nanoelectrode arrays without any loss of sensor sensitivity.

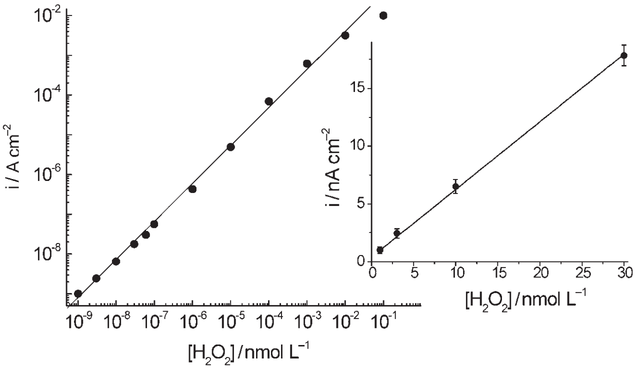

***Figure 3.*** Calibration plot of the sensor: peak-current density versus $H_2O_2$ concentration. Total amount of Prussian Blue: $\Gamma_{PB} \approx 10\,\mathrm{nmol\,cm^{-2}}$, operating potential: 50 mV, phosphate buffer (pH 6.0) + KCl (0.1 M), flow rate: $0.7\,\mathrm{mL\,min^{-1}}$. Inset: low-concentration limit of the calibration graph in linear coordinates.

The lower limit of the linear calibration range of the nanostructured $H_2O_2$ sensor (that is, $1\times10^{-9}\,\mathrm{mol\,L^{-1}}$ $H_2O_2$ (0.03 ppb), see Figure 3) is two orders of magnitude lower, and the upper limit (that is, $1\times10^{-2}\,\mathrm{mol\,L^{-1}}$ $H_2O_2$) is one order of magnitude higher, than those observed for conventional (unstructured) Prussian Blue.

An important analytical parameter is the sensor dynamic range. As can be seen, nanostructured Prussian Blue in the flow-injection mode displays a linear calibration range that extends over seven orders of magnitude of $H_2O_2$ concentration, and this range represents a record in electroanalysis.

## Experimental Section

Prussian Blue was electrodeposited from a solution of $K_3[Fe(CN)_6]$/$FeCl_3$ (4 mM each) in the supporting electrolyte, HCl/KCl (0.1 M each), by means of cyclic voltammetry at a sweep rate of 20–40 $\mathrm{mV\,s^{-1}}$ (switching potentials: 0.4 V (cathodic) and 0.7–0.8 V (anodic), see references [9,10]).

Nanostructuring was carried out by electrodepositing the electrocatalyst through sol templates of alkoxysilane (0.5–4 wt %), water (1.1–7.5 wt %), and an organic solvent (acetonitrile, 2-Propanol), and then drying it at room temperature. After deposition of the Prussian Blue, the sol template was removed using acetone.

Received: January 25, 2007
Revised: June 13, 2007

**Keywords:** electrochemistry · nanostructures · peroxides · Prussian Blue · sensors

[1] A. J. Bard, L. R. Faulkner, *Electrochemical methods. Fundamentals and applications*, 2nd ed., Wiley-VCH, Weinheim, **2001**, p 833.

[2] K. Aoki, *Electroanalysis* **1993**, *5*, 627–639.

[3] K. B. Oldham, *J. Electroanal. Chem.* **1981**, *122*, 1–17.

[4] R. Feeney, S. P. Kounaves, *Electroanalysis* **2000**, *12*, 677–684.

[5] G. C. Fiaccabrino, M. Koudelka-Hep, *Electroanalysis* **1998**, *10*, 217–222.

[6] C. Amatore, J. M. Saveant, D. Tessier, *J. Electroanal. Chem.* **1983**, *147*, 39–51.

[7] T. Gueshi, K. Tokuda, H. Matsuda, *J. Electroanal. Chem.* **1978**, *89*, 247–260.

[8] A. A. Karyakin, E. E. Karyakina, *Sens. Actuators B* **1999**, *57*, 268–273.

[9] A. A. Karyakin, E. E. Karyakina, L. Gorton, *Anal. Chem.* **2000**, *72*, 1720–1723.

[10] A. A. Karyakin, *Electroanalysis* **2001**, *13*, 813–819.

[11] G. S. Attard, P. N. Bartlett, N. R. B. Coleman, J. M. Elliott, J. R. Owen, J. H. Wang, *Science* **1997**, *278*, 838–840.

[12] G. S. Attard, P. N. Bartlett, N. R. B. Coleman, J. M. Elliott, J. R. Owen, *Langmuir* **1998**, *14*, 7340–7342.

[13] S. A. G. Evans, J. M. Elliott, L. M. Andrews, P. N. Bartlett, P. J. Doyle, G. Denuault, *Anal. Chem.* **2002**, *74*, 1322–1326.

[14] A. A. Karyakin, E. A. Puganova, I. A. Budashov, I. N. Kurochkin, E. E. Karyakina, V. A. Levchenko, V. N. Matveyenko, S. D. Varfolomeyev, *Anal. Chem.* **2004**, *76*, 474–478.

[15] J. Yamada, H. Matsuda, *J. Electroanal. Chem.* **1973**, *44*, 189–198.

[16] W. J. Albery, S. Bruckenstein, *J. Electroanal. Chem.* **1983**, *144*, 105–112.

[17] A. A. Karyakin, E. E. Karyakina, L. Gorton, *J. Electroanal. Chem.* **1998**, *456*, 97–104.

[18] J. Ruzicka, E. H. Hansen, *Flow injection analysis*, 2nd ed., Wiley, Ney York, **1988**.